



## ULTRASONIC SPECTROSCOPY OF SILICON SINGLE CRYSTAL

**Petr Sedlak<sup>1)</sup>, Pavel Tofel<sup>1)</sup>, Vlasta Sedlakova<sup>1)</sup>, Jiri Majzner<sup>1)</sup>, Josef Sikula<sup>1)</sup>,  
Lech Hasse<sup>2)</sup>**

1) Brno University of Technology, Faculty of Electrical Engineering and Communications, Department of Physics, Technicka 10, Brno 61600, Czech Republic (✉ sedlakp@feec.vutbr.cz)

2) Gdansk University of Technology, Faculty of Electronics, Telecommunications and Informatics, Department of Metrology and Optoelectronics, G. Narutowicza 11/12, 80-233 Gdańsk (lhasse@eti.pg.gda.pl)

### Abstract

Specimens of Si single crystals with different crystal orientation [100] and [110] were studied by Electro-Ultrasonic Spectroscopy (EUS) and Resonant Ultrasonic Spectroscopy (RUS). A silicon single crystal is an anisotropic crystal, so its properties are different in different directions in the material relative to the crystal orientation. EUS is based on interaction of two signals: an electric AC signal and an ultrasonic signal, which are working on different frequencies. The ultrasonic wave affects the charge carriers' transport in the structures and the intermodulation electrical signal which is created due to the interaction between the ultrasonic wave and charge carriers, is proportional to the density of structural defects. RUS enables to measure natural frequencies of free elastic vibrations of a simply shaped specimen by scanning a selected frequency range including the appropriate resonances of the measured specimens.

Keywords: non-destructive testing, silicon single crystal, electro-ultrasonic spectroscopy, resonant ultrasonic spectroscopy.

© 2011 Polish Academy of Sciences. All rights reserved

### 1. Introduction

The number of manufactured electric component increases with every year as well as the requirements on their quality and reliability. Electro-Ultrasonic Spectroscopy (EUS) [1] and Resonant Ultrasound Spectroscopy (RUS) [2] belong to a group of new promising techniques for non-destructive testing of electronic components.

EUS is based on interaction of two signals: an electric AC signal and an ultrasonic signal, which are excited on different frequencies. The ultrasonic wave affects the charge carriers' transport in the structures and the intermodulation electrical signal which is created due to the interaction between the ultrasonic wave and charge carriers, is proportional to the density of structural defects. The ultrasonic phonons influence the transport of electrons, where the intermodulation of ultrasonic and electric current frequencies appears in the vicinity of defects. Thus, a new harmonic signal appears on the differential frequency of the exciting signals. It is the result of the electrical resistance change due to the variation of the inhomogeneity effective area by ultrasonic excitation [3, 4].

The RUS measurement system generates a harmonic signal at a given frequency and measures the amplitude of vibrations of an object that was placed between the transmitter and the receiver. The system measures the vibration spectrum by sweeping the frequency of the stimulated harmonic with an appropriate resolution [5]. As a result the experiment enables to achieve the resonant spectrum of a free oscillating object body. Variations in the internal

object structure imply differences of its mechanical properties (e.g. in sound velocity and, consistently, in resonant frequencies) due to the presence of some imperfections in the sample microstructure, namely impurities, inhomogeneous strain and crystallographic defects such as dislocations that can be identified by the convenient RUS procedure.

In the paper, the crystal properties were measured by ultrasonic spectroscopy techniques. The experimental study is performed on a Si single crystal of total dimension  $3.0 \times 3.0 \times 30.0 \text{ mm}^3$ . The specimens were prepared in cooperation with Dr. Young H. Kim from the Korea Science Academy [6]. The 3 inches diameter and 3 mm thickness of p-type silicon-boron wafers in the [100] and [110] directions were sliced by using a low-speed diamond wheel saw, so that the direction of length are in directions [110] and [100]. The resistivity of the original wafers was  $14.4 \text{ } \Omega\text{cm}$ . Electrodes for a 4-point probe were provided on the specimen. The distance between probing electrodes was 26 mm. Fig. 1 shows the positions of four contacts and the sample.

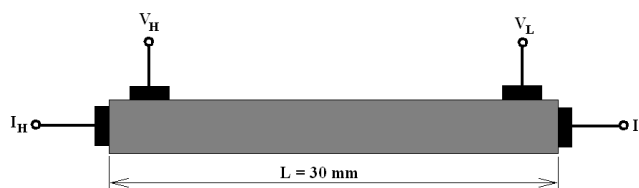


Fig. 1. Si single crystal [110] of dimension  $3.0 \times 3.0 \times 30.0 \text{ mm}^3$ ; electric resistance between current contacts is  $3.7 \text{ k}\Omega$  and between voltage contacts is  $2.19 \text{ k}\Omega$ .

## 2. Electro-Ultrasonic Spectroscopy

The method can be used as a diagnostic tool for quality and reliability assessment. It is sensitive to the decrease of charge carrier mobility caused by various defects in material structure. The sample is excited by two independent sources: a Langevin ultrasonic transducer working on frequency  $f_U$  and the harmonic electrical signal of frequency  $f_E$  which is close to the ultrasonic source. A new harmonic signal of the frequency  $f_i$  is created as a result of the electrical resistance change due to the variation of the crack effective area by ultrasonic excitation. The intermodulation frequency  $f_i$  is given by the subtraction or addition of excitation frequencies  $f_E$  and  $f_U$ .

The wavelength of the ultrasonic signal is greater than mean free path of carriers, thus, the ultrasonic signal has no influence on the carriers directly. Ultrasonic vibrations impact the geometry of the sample as well as the geometry of defects. These defects and other impurities in material structure represent the boundaries on which additional sources of resistance change are created. Thus the resistance change of such sample will be more significant than in a pure material. Considering a crack in the sample, the resistance change corresponding to this crack depends on several factors, such as crack size, crack shape, its orientation against the direction of the ultrasonic wave etc.

As mentioned above, the method uses an AC electrical signal of frequency  $f_E$  and the ultrasonic signal of frequency  $f_U$ . In this case, the classical mixing modulation principle with two harmonic components is applied, thus, the signal giving information on the sample electrical conductivity has the frequency  $f_i = f_E \pm f_U$ , which is different from the frequencies of both exciting signals.

We assume that the measured voltage across the sample  $V_T$  is given by the electric current flowing through the sample and ultrasonic excited resistance change:

$$V_T = f[i_{AC}(f_E), \Delta R(f_U)], \quad (1)$$



where  $i_{AC}$  is the amplitude of the electric AC current,  $f_E$  and  $f_U$  denote the frequency of electric and ultrasonic excitation, respectively.  $\Delta R$  represents the amplitude of resistance change due to the ultrasonic excitation.

Firstly, we consider only electrical excitation. The measured sample of resistance  $R_{DUT}$  and protective resistor  $R_P$  are connected to an electric generator, as shown in Fig. 2 a. Protective resistor  $R_P$  and the generator are the source of electric current  $i_{AC}$ , (Fig. 2 b). The voltage  $V_T$  measured on the sample is:

$$V_T = R_{DUT} \cdot i_{AC} \cos(\omega_E t), \quad (2)$$

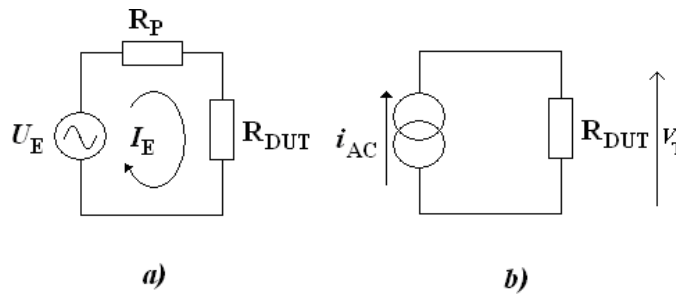


Fig. 2. Equivalent electrical circuit from figure 1, a) model with voltage source, b) simplified model with current source.

Further, we fix the sample on the ultrasonic actuator that generates the ultrasonic signal of frequency  $f_U$ . The resistance of the sample is changing with the amplitude  $\Delta R$ , and is also varying with frequency  $f_U$ , (Fig. 3). Thus, the voltage  $V_T$  measured across the sample is given by:

$$V_T = (R_{DUT} + \Delta R) \cdot i_{AC} \cos(\omega_E t), \quad (3)$$

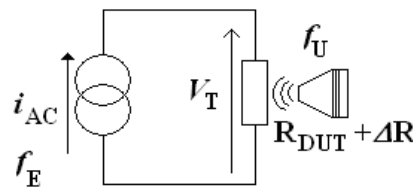


Fig. 3. Electric circuit and ultrasonic transducer that influences the sample resistance.

The resistance change  $\Delta R$  depends on the mean amplitude of the mechanical vibration  $A(\omega_U)$  of the ultrasonic actuator:

$$A(\omega_U) = H(\omega_U) \cdot V_U \cdot \cos(\omega_U t), \quad (4)$$

where  $V_U$  is the voltage of the generator for ultrasonic excitation and  $H(\omega_U)$  is the transfer function of the ultrasonic part of the measurement setup (i.e. generator, power amplifier, ultrasonic actuator, bonding between the actuator and specimen). Thus, the resistance change  $\Delta R$  is given by:

$$\Delta R = k_U(\omega_U) \cdot A(\omega_U) = k_U(\omega_U) \cdot H(\omega_U) \cdot V_U \cos(\omega_U t) = \Delta R_M \cdot \cos(\omega_U t), \quad (5)$$

where  $k_U(\omega_U)$  represents the transfer function of the specimen and depends on several factors, such as material, geometry, temperature and concentration of defects. The voltage  $V_T$  is:

$$V_T = (R_{DUT} + \Delta R) \cdot i_{AC} \cos(\omega_E t) = [R_{DUT} + k_U(\omega_U) \cdot H(\omega_U) \cdot V_U \cos(\omega_U t)] \cdot i_{AC} \cos(\omega_E t) = R_{DUT} \cdot i_{AC} \cos(\omega_E t) + \frac{1}{2} k_U(\omega_U) \cdot H(\omega_U) \cdot V_U \cdot i_{AC} [\cos(\omega_E t - \omega_U t) + \cos(\omega_E t + \omega_U t)] \quad (6)$$

The theoretical voltage spectrum, which is given by equation (6), consists of three frequency components, as presented in Fig. 4. The voltage at frequency  $f_E$  is given by the resistance of the sample  $R_{DUT}$  and the AC current flowing through the sample. Sideband components correspond to the voltage that is determined by resistance change  $\Delta R$  and AC current flowing through the sample structure.

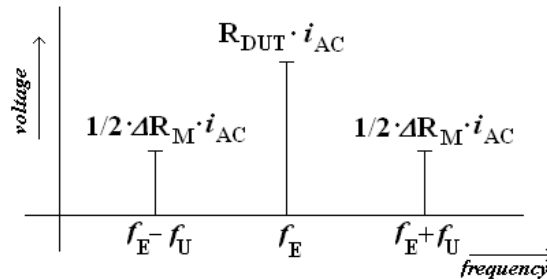


Fig. 4. EUS theoretical spectrum given by equation (6).

### 2.1. Expected sensitivity of EUS measurement setup

To reach a high resolution of the EUS technique, the AC generator should have features such as low-background noise and the signal-to-noise ratio (SNR) higher than 100 dB in the pass-band near the intermodulation frequency. Since the noise background of the measured signal increases with the bandwidth of the amplifier, it is necessary to optimize the frequency band of the amplifier with respect to the signal-to-noise ratio [7].

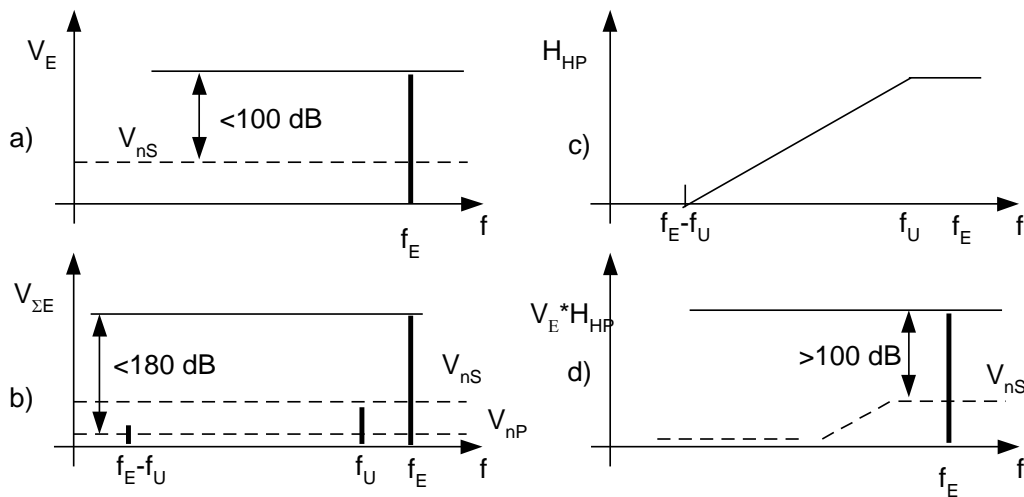


Fig. 5. Signals and noise of the AC generator in the frequency domain a) the electrical exciting signal at frequency  $f_E$  and noise background  $V_{nS}$  (standard generator SNR is about 100 dB), b) SNR in DUT, c) frequency response of HP filter, d) signal and noise after filtration.

The measurement setup contains of a high-pass filter (HP filter) to increase the AC generator SNR up to 180 dB. The HP filter transmits the exciting signal at frequency  $f_E$ , and attenuates the noise in the low-frequency band, where the useful signal at the intermodulation



frequency  $f_i$  is measured. Fig. 5c shows the frequency response of the HP filter. Fig. 5a represents the exciting signal which is generated by the AC generator, before the filtration process while Fig. 5d represents the same signal after the filtration. Since the signal is led from the power amplifier to the input of the HP filter, the filter has to be designed for high voltage and a high current load.

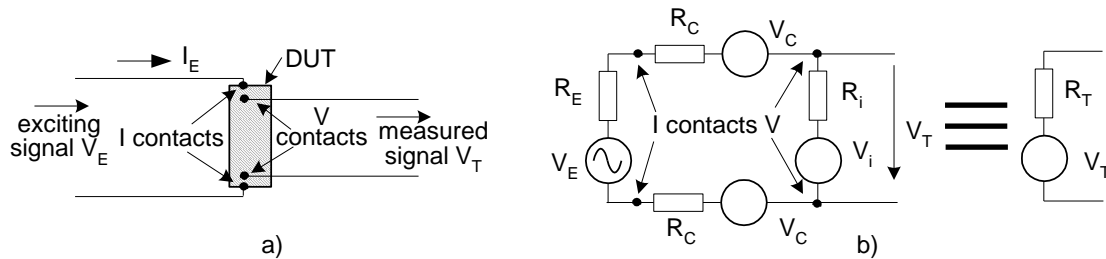


Fig. 6. Four-probe method: a) circuitry, b) equivalent DUT electrical diagram:  $V_E$  and  $R_E$  - exciting generator parameters,  $V_C$  and  $R_C$  - parameters that cover noise and parasitic modulation of current contacts,  $V_i$  and  $R_i$  - source of inter-modulated signal on the defect,  $V_T$  - measured signal.

It should be considered that the current contacts on the device under test (DUT) could be the source of a parasitic modulated signal which is similar to the signal caused by the defects in the measured structure. Then it is suitable to use four-point connection with current and voltage contacts, where the main current flow through the current contacts is as presented in Fig. 6a. On the voltage contacts the signal at the intermodulation frequency corresponds to the change of the DUT resistance without the parasitic-modulation effect due to the contacts, as shown schematically in Fig. 6b. Resistances  $R_i$ , which is related to the measured sample, and  $R_C$ , which is related to the contact region, are considered to be much lower than the internal resistance  $R_E$  of the AC source. Therefore the transfer of the parasitic voltage  $V_C$  to the voltage  $V_T$  is much lower than 1, because it is proportional to the ratio given by the resistance division  $R_i / (R_i + 2R_C + R_E)$ . This parasitic effect of contacts could be minimized by proper soldering or by using other mechanical connections.

The changes of the electrical resistance caused by ultrasonic excitation are very small. Thus, it is necessary to evaluate the basic sensitivity of the EUS technique. The limiting factors are the noise of the load resistance, preamplifier noise and noise due to the temperature fluctuation caused by the high current density in DUT.

We estimate the maximum sensitivity of our proposed EUS method. Thevenin's model of the measured signal source  $V_T$  has an internal resistance  $R_T$  (see Fig. 6b)), which can be expressed as the parallel combination of resistance  $R_i$  and load resistance ( $R_E + 2R_C$ ). Because the resistance  $R_i \ll R_E$ , the value of resistance  $R_T$  is very low (similar to  $R_i$ ). We may consider the internal resistance  $R_T$  value in the range (0.01 – 1)  $\Omega$ . For a resistance  $R = 1 \Omega$  and temperature  $T = 300 \text{ K}$ , the thermal noise spectral density  $S_{ne}$  is given by:

$$S_{ne} = 4kTR = 1.6 \times 10^{-20} \text{ V}^2/\text{Hz}, \quad (7)$$

where  $k$  is the Boltzmann constant. Then, the noise voltage  $V_n$  is:

$$V_n = \sqrt{S_{ne} \cdot B}, \quad (8)$$

where  $B$  is the effective noise pass-band. Considering a pass-band of  $B = 100 \text{ Hz}$ , the effective noise voltage of the load resistance is equal to  $V_n = 1.2 \text{ nV}$ . This value is lower than the background noise of the preamplifier. In this case, the noise voltage of the preamplifier determines the basic sensitivity of the EUS technique. The resultant noise could be essentially limited by reducing the  $B$  value as well as preamplifier noise voltage. For a low-noise

preamplifier of  $V_{ne} = 1 \text{ nV}/\sqrt{\text{Hz}}$  and a pass-band  $B = 100 \text{ Hz}$ , the equivalent noise voltage  $V_n$  equals  $10 \text{ nV}$ . Considering the voltage  $V_T = 0.1 \text{ V}$ , the detectable relative value of the resistance change can be expressed as

$$\Delta R / R_{\text{DUT}} = V_n / V_T = 1 \times 10^{-8} / 0.1 = 1 \times 10^{-7}. \quad (9)$$

Since source resistance  $R_T$  is of the order of  $0.1 \Omega$  and preamplifier noise resistance is  $10^3$  to  $10^4$  times greater, the sensitivity can be increased from 30 to 100 times by using a transformer. On the basis of these conclusions, we estimate the maximum sensitivity of the proposed electro-ultrasonic spectroscopy method at 120 to 160 dB, approximately.

The measurement method is based on the mixing principle, where the resultant voltage  $V_T$  contains following spectral components

$$f_i = |\pm n f_E \pm m f_U|_{n,m=0,1,2,\dots}. \quad (10)$$

Since a linear parametric mixing system is considered, the intermodulation frequency  $f_i$  is derived by the superposition or subtraction of exciting frequencies  $f_E$  and  $f_U$ . It holds

$$f_i = f_E - f_U \quad \text{or} \quad f_i = f_E + f_U. \quad (11)$$

There are two methods of signal detection in (i) The low-frequency band for  $f_i = f_E - f_U$  and (ii) The high-frequency band for  $f_i = f_E + f_U$ . The main advantage of EUS lays in the fact that the intermodulation component of the electrical signal is at a completely different frequency from the frequencies of both exciting sources. This fact allows us to reach a high signal-to-noise ratio and to design a NDT method with high resolution and high sensitivity to defects in the DUT. The electrical excitation (at frequency  $f_E$ ) has a high amplitude in comparison with the intermodulation signal that requires an amplifier with a high dynamic range. The low-pass (LP) filter, which possesses a cut-off frequency slightly higher than  $f_i$  and a sufficient rejection level, is used to solve the problem of the high dynamic range for signal processing. Thus, the frequency spectrum is obtained with lower dynamic range, which can be amplified by a low noise preamplifier and measured by a selective nanovoltmeter, filtered by a band-pass filter or by FFT analyses.

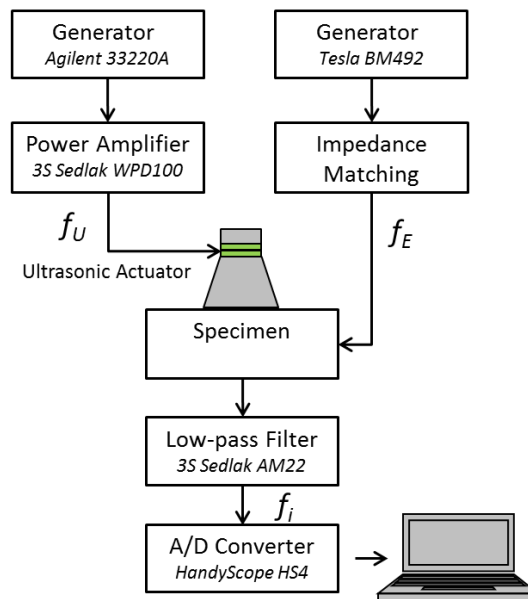


Fig. 7. Scheme of the experimental setup for electro-ultrasonic spectroscopy.

## 2.2. Experimental setup

Fig. 7 shows the scheme of our experimental setup. The ultrasonic part consists of an Agilent 33220A generator. The power amplifier is a WPD 100 (3S Sedlak, Inc.) from which it is necessary to have a power linear actuating harmonic signal on the ultrasonic transducer. The measured sample was fixed on a Langevin ultrasonic transducer (HTP04, 3S Sedlak, Inc.) which is used for ultrasonic signal generation. The electric part consists of a Tesla BM492 generator which has proper linearity and frequency stability. A low-pass filter and low-noise amplifier (AM22, 3S Sedlak, inc.) were employed to acquire the intermodulation signal.

Waveforms of the intermodulation signal were captured by using an A/D converter and frequency components were obtained by using an FFT algorithm which calculates power spectral density. Magnitudes of the intermodulation signal were determined from the peaks of the estimated power spectral densities.

## 2.3. Results and discussion

In order to obtain the maximal value of the intermodulation signal, the ultrasonic excitation frequency was tuned to reach the resonant frequency of the system formed by the actuator + sample. The electrical excitation frequency was set to obtain the intermodulation frequency at 2 kHz. Thus, measurements were performed on an ultrasonic signal of frequency  $f_U = 31.9$  kHz and for an electric signal of frequency  $f_E = 33.9$  kHz.

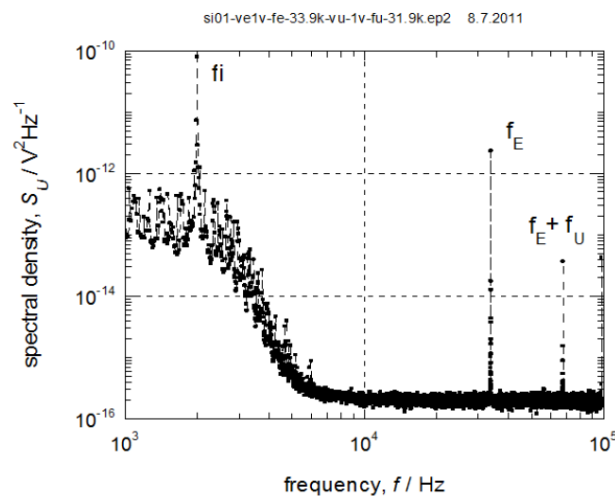


Fig. 8. Typical power spectral density of the measured sample.  $f_U = 31.9$  kHz and  $f_E = 33.9$  kHz.

Fig. 8 shows the typical power spectral density measured on the Si specimen with direction [100], where the peaks of the intermodulation signal and electrical excitation are clearly visible. The noise background of the measurement setup is of the order of  $1.10^{-13} \text{ V}^2 \text{ Hz}^{-1}$ .

For the evaluation of measurements, the amplitude of the intermodulation signal is given by

$$V_i = \sqrt{S_U \Delta f} \quad (7)$$

where  $S_U$  denotes the value of the power spectral density, which was measured at the intermodulation frequency, and  $\Delta f$  is the frequency resolution [8, 9].



Fig. 7 presents, in four measured dependencies, the intermodulation voltage in dependence on the amplitudes of ultrasonic excitation and electrical excitation for Si specimens in both longitudinal directions ([100] and [110]). As the amplitude of ultrasonic excitation or the amplitude of electrical excitation increases, the intermodulation component increases as well. The slope of each measured dependence is  $m = 1$ , which we expected since the modulation amplitude is linearly proportional to the change of resistance by ultrasonic excitation. Fig. 9 also shows saturation once the ultrasonic voltage exceeded a certain value. This saturation may occur in every specimen when the ultrasonic excitation ceases to influence the flow of electrical current through the specimen. The saturation depends on the material structure, contact quality and electrical excitation.

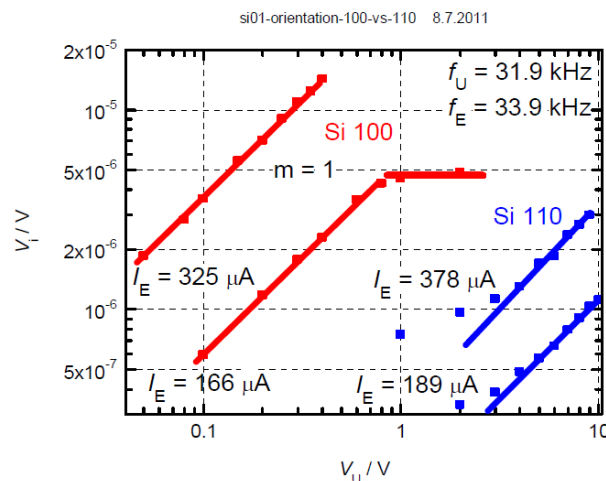


Fig. 9. Intermodulation voltage as a function of ultrasonic excitation and electrical excitation for Si specimens of both direction ([100] and [110]).

Further, these measurements reveal that a Si specimen of longitudinal direction [100] is more sensitive than a specimen of direction [110]. Thus, it implies that EUS can give us information not only about nonlinearities in the structure but also about the structure itself.

### 3. Resonant Ultrasonic Spectroscopy

The RUS experiment used to characterize a material anisotropy generates a resonance spectrum that contains much information, but extracting all that information is not an easy task. Measured samples can be mounted between two transducers at opposite corners with minimal pressure. One transducer excites the measured specimen and the other one measures its response (Fig. 10a). Part of the mechanical construction of the system is shown in Fig. 10b.

A harmonic signal with swept frequency is applied to the input of the sensor, exciting vibrations in the tested crystal closed into a specially shielded box padded with cork as an anti-vibration isolating material. Signals of both sensors were amplified by two independent amplifiers; the receiving preamplifier was working as a charge amplifier and its inherent noise is negligible. The National Instrument NI PCI 5406 was used as the stimulating generator, and the output signal from the receiving preamplifier was applied to the NI PCI 6132 DAQ through the NI BNC 2110 connector enabling signal processing up to 3 MHz/s/channel. The whole system was working under LabVIEW control. It enables to set the amplitude of the stimulus signal, the frequency range of measurement and the frequency sweeping step, what gives an appropriate spectrum resolution.



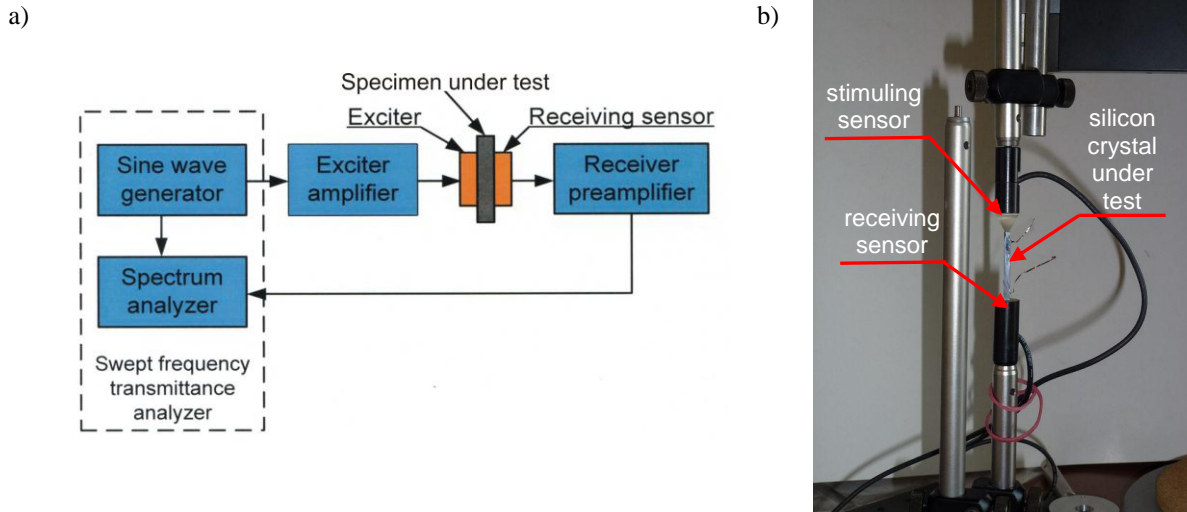


Fig. 10. General simplified block diagram of the system for resonant ultrasound spectroscopy (a) and the part of the mechanical construction with a measured silicon crystal (b).

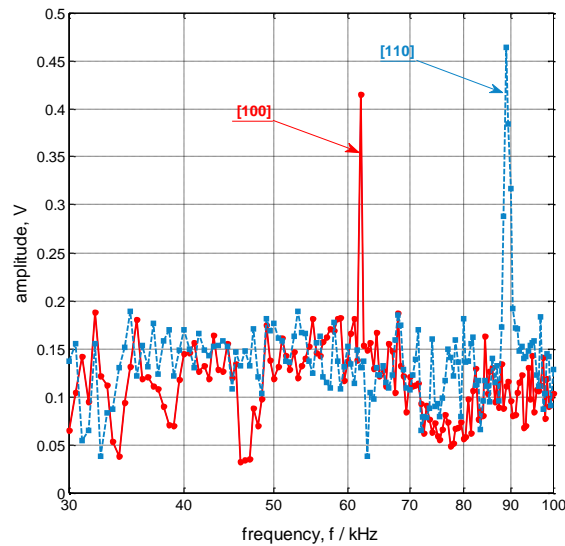


Fig. 11. Resonant ultrasound spectrum of vibrations obtained for the tested silicon crystal samples with orientation [100] (red lines, circles) and [110] (blue lines, squares).

The Young's modulus of a material is an important parameter of its mechanical properties enabling to quantify the elastic behavior of the material. Silicon is an anisotropic crystalline material whose properties depend on orientation relative to the crystal lattice. Monocrystalline silicon is highly structured; its structure has cubic symmetry. For an anisotropic material its elastic behavior depends on the orientation of the structure, in which crystal direction the material is being stretched. It is well known that Young's (elasticity) modulus varies significantly for silicon [100] and [110] from about 130 GPa to 188 GPa, respectively [10].

A free vibrating body of the measured object can sustain vibrations at several resonant frequencies related to the elastic constants and specimens geometry being internal variables of the Lagrangian [2]. To identify various vibration modes one can use the extracting procedure comparing the measured frequencies with computed ones.

Measured silicon crystal samples with the same geometrical dimensions exhibited an evident resonance at a low frequency below 100 kHz. However there was a significant

difference in this resonance frequency for a sample with [100] orientation compared with the results for [110] samples (Fig. 9). A shift of the resonance frequency to a lower value for the sample with [100] orientation had been observed. It corresponds to the different values of elastic constants of the specimens with different crystallographic orientation. It means that the RUS can indicate additionally the orientation of a crystal structure, not only its inhomogeneities related to possible cracks and other defects in a specimen.

#### 4. Conclusions

Specimens of Si single crystals with different crystal orientation [100] and [110] were studied by electro-ultrasonic spectroscopy and resonant ultrasonic spectroscopy. These techniques give a possibility to differentiate between crystal orientation and eventually some defects in measured specimens. Additionally, both techniques can give also information on material structure, not only about defects.

#### Acknowledgment

This research was partially financed by the Czech-Polish project MEB 051003 and 8057/2010 as well as by the Grant Agency of Czech Republic No. 102/09/1920.

#### References

- [1] Hajek, K., Sikula, J. (2007). The improved system for electro-ultrasonic nonlinear spectroscopy. In *Proceeding of NDT in Progress 2007*, Prague, Czech Republic, 71-79.
- [2] Migliori, A., Sarrao, J.L. (1997). *Resonant Ultrasound Spectroscopy*. J. Wiley & Sons.
- [3] Sedlakova, V., Sikula, J., Tofel, P., Majzner, J. (2008) Electro-ultrasonic spectroscopy of polymer based thick film layers. *Microelectronics Reliability*, 48(6), 886-889.
- [4] Sedlakova, V., Sikula, J., Tofel, P. (2007). Electro-ultrasonic spectroscopy of conducting solids. In *Proceedings of IMAPS Poland 2007*, Rzeszów-Krasiczyn, Poland, 523-525.
- [5] Hasse, L., Kwiłczo, M., Smulko, J., Stepinski, T. (2009). Quality assessment of varistor ZnO structures by resonant ultrasound spectroscopy. *Insight*, 51(5), 262-265.
- [6] Kim, Y.H., Han, M., Sedlakova, V., Sikula, J. (2010) Feasible study on electro-ultrasonic spectroscopy of silicon single crystal. In *Proceeding of Symposium on Ultrasonic Electronics*, Tokyo, Japan, 301-302.
- [7] Sikula, J., Hajek, K., Sedlakova, V.; Tofel, P., Majzner, J (2008) Improved Signal to Noise Ratio of Electro-ultrasonic Spectroscopy. *ElectroScope*, 2(6), 1-4.
- [8] Hajek, K., Sikula, J., Sedlak, P. (2004), Improving the practical sensitivity of nonlinear ultrasound spectroscopy for one exciting signal. In *Proceeding of Defektoskopie 2004*, Spindleruv Mlyn, Czech Republic, 51-58. (in Czech)
- [9] Tofel, P., Sikula, J., Sedlakova, V. (2009) NDT of single crystal CdTe and Si by electro-ultrasonic spectroscopy. In *Proceeding of NDT in Progress 2009*, Prague, Czech Republic, 305.
- [10] Hopcroft, M., Nix, W., Kenny, T. (2010) What is the Young's Modulus of Silicon? *Journal of Microelectromechanical Systems*, 19, 229-238.

